Oxidative stress is a consequence, not a cause, of aluminum toxicity in the forage legume *Lotus corniculatus*

Joaquín Navascués[1], Carmen Pérez-Rontomé[1], Diego H. Sánchez[2], Christiana Staudinger[3], Stefanie Wienkoop[3], Rubén Rellán-Álvarez[1] and Manuel Becana[1]

[1]Departamento de Nutrición Vegetal, Estación Experimental de Aula Dei, Consejo Superior de Investigaciones Científicas, Apartado 13034, 50080 Zaragoza, Spain; [2]Max Planck Institute for Molecular Plant Physiology, Wissenschaftspark Golm, Am Mühlenberg 1, Potsdam-Golm, 14476, Germany; [3]Department of Molecular Systems Biology, University of Vienna, 1090 Vienna, Austria

Summary

- Aluminum (Al) toxicity is a major limiting factor of crop production on acid soils, but the implication of oxidative stress in this process is controversial. A multidisciplinary approach was used here to address this question in the forage legume *Lotus corniculatus*.
- Plants were treated with low Al concentrations in hydroponic culture, and physiological and biochemical parameters, together with semiquantitative metabolic and proteomic profiles, were determined.
- The exposure of plants to 10 μM Al inhibited root and leaf growth, but had no effect on the production of reactive oxygen species or lipid peroxides. By contrast, exposure to 20 μM Al elicited the production of superoxide radicals, peroxide and malondialdehyde. In response to Al, there was a progressive replacement of the superoxide dismutase isoforms in the cytosol, a loss of ascorbate and consistent changes in amino acids, sugars and associated enzymes.
- We conclude that oxidative stress is not a causative factor of Al toxicity. The increased contents in roots of two powerful Al chelators, malic and 2-isopropylmalic acids, together with the induction of an Al-activated malate transporter gene, strongly suggest that both organic acids are implicated in Al detoxification. The effects of Al on key proteins involved in cytoskeleton dynamics, protein turnover, transport, methylation reactions, redox control and stress responses underscore a metabolic dysfunction, which affects multiple cellular compartments, particularly in plants exposed to 20 μM Al.

Introduction

Aluminum (Al) toxicity is a major constraint of agricultural production on acid soils (pH < 5.6). In tropical America, acid soils cover nearly 850 million hectares (Rao *et al.*, 1993) and, in Brazil, 32% exhibit Al toxicity (Abreu *et al.*, 2003). In acid soils, Al is solubilized into soil solution from aluminosilicates, inhibiting root growth and function (Ma *et al.*, 2001; Kochian, 2005). At the cellular level, the strong binding affinity of Al with oxygen donor ligands, such as proteins, nucleic acids and phospholipids, results in the inhibition of cell division, cell extension and transport (Mossor-Pietraszewska, 2001). At the molecular level, Al stress causes major changes in the expression patterns of genes, some of which are important in the oxidative stress response (Richards *et al.*, 1998; Watt, 2003; Maron *et al.*, 2008). Indeed, exposure of plants to Al elicits the production of reactive oxygen species (ROS), which may cause oxidative damage to cellular components if antioxidant defenses are overwhelmed (Cakmak & Horst, 1991; Boscolo *et al.*, 2003; Darkó *et al.*, 2004; Sharma & Dubey, 2007). Major antioxidants in plants include catalases, superoxide dismutases (SODs), glutathione peroxidases (GPXs)

and the enzymes and metabolites of the ascorbate–glutathione pathway. This pathway ultimately reduces H_2O_2 to water at the expense of NAD(P)H, and involves four enzymes: ascorbate peroxidase (APX), monodehydroascorbate reductase (MR), dehydroascorbate reductase (DR) and glutathione reductase (GR).

The capacity of plants to overcome Al stress involves diverse mechanisms, one of which is the root exudation of organic acids and phenolic compounds (Pellet *et al.*, 1995; Ma *et al.*, 2001; Barceló & Poschenrieder, 2002). The discovery and characterization of an Al-activated malate transporter (ALMT) provide genetic support for an important role of organic acids in withstanding Al toxicity (Sasaki *et al.*, 2004; Hoekenga *et al.*, 2006). In addition, the use of large-scale ('omics') technologies has contributed considerably to our understanding of the effects and mechanisms of Al toxicity. This is exemplified by very recent transcriptomic (Kumari *et al.*, 2008; Maron *et al.*, 2008; Eticha *et al.*, 2010) and proteomic (Yang *et al.*, 2007; Zhen *et al.*, 2007; Zhou *et al.*, 2009) studies. However, to our knowledge, the effects of Al stress have not yet been addressed using metabolic profiling or semiquantitative proteomics. Moreover, the implication of oxidative stress as a primary mechanism of Al toxicity is still controversial.

Several authors have associated Al toxicity with the induction of oxidative stress (Richards *et al.*, 1998; Ezaki *et al.*, 2000; Sharma & Dubey, 2007), whereas others have proposed that the oxidation of lipids or proteins (markers of oxidative stress) is not directly responsible for the inhibition of root elongation caused by Al (Cakmak & Horst, 1991; Yamamoto *et al.*, 2001; Boscolo *et al.*, 2003). A complicating factor in this controversy is that the increase in antioxidant enzyme activities and ROS production is often interpreted as being indicative of oxidative stress (e.g. Darkó *et al.*, 2004), although these molecules may be involved in 'oxidative signaling' under conditions that do not necessarily imply damage to cellular components, and hence oxidative stress (Foyer & Noctor, 2005).

Forage legumes play an important role in the productivity of cultivated pastures because of their high potential for N_2 fixation and growth in soils with low fertility. In particular, *Lotus corniculatus* has an outstanding agricultural importance and wide distribution in South America (Díaz *et al.*, 2005), and is closely related to *L. japonicus*, a model species for classical and molecular genetics (Handberg & Stougaard, 1992). Previous work has shown that exposure to high Al concentrations triggers a rapid membrane depolarization in *L. corniculatus* root cells, suggesting a role of this process in the inhibition of root cell elongation (Pavlovkin *et al.*, 2009). Here, we have investigated the implication of oxidative stress in Al toxicity in *L. corniculatus* using a multidisciplinary approach. Measurements of physiological and biochemical parameters, in combination with semiquantitative analyses of the metabolome and proteome of roots, were performed to identify the metabolic and cellular processes involved in the long-term response of plants to physiologically relevant Al concentrations.

Materials and Methods

Biological material and plant treatments

Seeds of *Lotus corniculatus* L. cv Draco were surface disinfected with 70% ethanol, transferred to 0.5% agar plates and stored at 4°C for 2 d. Germinating seeds were then incubated at 28°C for 2 d and placed on 1.5% agar plates (8–10 seedlings per plate; Supporting Information Fig. S1a) containing a complete nutrient medium (modified Fahraeus medium; Boisson-Dernier *et al.*, 2001). After 1 wk, seedlings were transferred to 10-l hydroponic vessels containing deionized water with 200 μM $CaCl_2$ and 0, 10 or 20 μM $AlCl_3$ (adjusted to pH 4.0) in a controlled environment cabinet (ASL, Madrid, Spain) under the following conditions: 23°C : 18°C (day : night), 70% relative humidity, 180 μmol m^{-2} s^{-1} and a 16-h photoperiod. Plants were harvested after 14 d (Fig. S1b), and roots and leaves were snap-frozen in liquid nitrogen and stored at $-80°C$.

Accumulation of Al and production of ROS

The accumulation of Al in roots was visualized using morin (2′,3,4′,5,7-pentahydroxyflavone; Fluka, Buchs, Switzerland), which forms a highly specific complex with Al at acidic pH. The method of Tice *et al.* (1992) was followed with minor modifications. Roots were washed six times (30 min each) with desorbing

solution (1 mM sodium citrate, 5 mM $CaCl_2$, pH 4.0) and frozen for 6 h. Roots were then thawed, washed four times for 30 min each in desorbing solution, washed in buffer (5 mM ammonium acetate, pH 5.0) for 10 min, stained with 100 μM morin in buffer for 60 min and washed again in buffer for 10 min.

The production of ROS in roots was visualized using specific fluorescent probes (Sandalio *et al.*, 2008). To detect superoxide radical formation, roots were preincubated with 100 μM $CaCl_2$ for 30 min, incubated with 10 μM dihydroethidium (DHE; Sigma-Aldrich) in 100 μM $CaCl_2$ for 30 min, and finally washed with 100 μM $CaCl_2$. DHE is oxidized by superoxide radicals to oxyethidium, which is quite stable and fluoresces with excitation at 488 nm and emission at 520 nm. To detect peroxide production, roots were processed as indicated for superoxide radicals, but replacing DHE by 25 μM of 2′,7′-dichlorofluorescein diacetate (DCF-DA; Calbiochem, Darmstadt, Germany). This compound is able to permeate cells, where it is hydrolyzed by intracellular esterases releasing DCF, which becomes trapped inside the cell. DCF reacts with H_2O_2 and hydroperoxides forming a fluorescent compound with excitation at 480 nm and emission at 530 nm (Sandalio *et al.*, 2008).

Roots were examined using an M165 FC fluorescence stereomicroscope (Leica, Wetzlar, Germany) with a GFP3 filter (excitation 450–490 nm, emission 500–550 nm) for Al and peroxides, and with a DSR filter (excitation 510–560 nm, emission 590–650 nm) for superoxide radicals.

Physiological parameters and oxidative stress markers

Plant growth was assessed by measurement of the leaf and root fresh weight (FW), leaf area and root length. The root and leaf contents of nitrogen (N) were determined with an NA 2100 Nitrogen Analyzer (ThermoQuest, Milan, Italy). The root and leaf contents of Al were measured by inductively coupled plasma-mass spectrometry (ICP-MS) with an ELAN 6000 instrument (Perkin-Elmer, Waltham, MA, USA) at the Universidad Autónoma de Barcelona (Spain). The root contents of potassium (K), calcium (Ca), magnesium (Mg), phosphorus (P), sulfur (S), iron (Fe), copper (Cu), manganese (Mn), nickel (Ni) and zinc (Zn) were measured by inductively coupled plasma-atomic emission spectroscopy (ICP-AES) with an IRIS Intrepid II XDL instrument (Thermo Electron, Waltham, MA, USA) at CEBAS-CSIC (Murcia, Spain). All metals and other elements were extracted from plant tissues and quantified according to standard protocols.

The oxidative damage of lipids was estimated as the content of malondialdehyde, a cytotoxic aldehyde produced during lipid peroxidation. Briefly, the method involved the extraction of malondialdehyde with 5% metaphosphoric acid containing 0.04% butylhydroxytoluene, and subsequent reaction with thiobarbituric acid at low pH and 95°C to form (thiobarbituric acid)$_2$–malondialdehyde adducts. These were extracted with 1-butanol and quantified by high-performance liquid chromatography (HPLC) with photodiode array detection (Iturbe-Ormaetxe *et al.*, 1998). The identity of the malondialdehyde adduct was verified by scanning of the peak and by co-elution with a standard of 1,1,3,3-tetraethoxypropane (Sigma-Aldrich).

Gene expression

Total RNA was extracted with the RNAqueous isolation kit (Ambion, Austin, TX, USA) and treated with DNaseI (Roche) at 37°C for 30 min. cDNA was synthesized from DNase-treated RNA with $(dT)_{17}$ and Moloney murine leukemia virus reverse transcriptase (Promega). Quantitative reverse transcription-polymerase chain reaction (qRT-PCR) analysis was performed with an iCycler iQ instrument using iQ SYBR-Green Supermix reagents (Bio-Rad) and gene-specific primers, as indicated previously (Rubio *et al.*, 2007). For the *ALMT* gene, the following primers were used: 5′-AGGTGCAACACTCAGCAA-AAGC-3′ (forward) and 5′-TGACCTCCAACCCCTAAAGCA-3′ (reverse). The PCR program and other details have been described previously (Rubio *et al.*, 2007). The amplification efficiency of primers, calculated using serial dilutions of root cDNAs, was > 75%, except for the primers of the genes encoding peroxisomal APX (APXpx), cytosolic GR (GRc), plastidic GR (GRp) and ALMT, whose efficiencies were > 65%. Expression levels were normalized using *ubiquitin* as the reference gene. Threshold cycle values were in the range of 17–19 cycles for *ubiquitin* and 22–29 cycles for the genes of interest. Three additional reference genes were used to confirm the stability of the *ubiquitin* transcript during Al stress. These genes encode the PP2A regulatory subunit, eukaryotic initiation factor 4A and glycosylphosphatidylinositol (GPI)-anchored protein, and have been selected, together with *ubiquitin*, from the most stably expressed genes in plants under a variety of stressful conditions (Czechowski *et al.*, 2005; Sánchez *et al.*, 2008). A comparison of their mRNA levels confirmed their stability in roots treated with 10 or 20 μM Al.

Antioxidant enzymes and metabolites

The SOD enzymes were extracted from roots with 50 mM potassium phosphate buffer (pH 7.8), 0.1 mM EDTA, 0.1% Triton X-100 and 1% polyvinylpyrrolidone-10 (PVP-10), and their activities were determined by the ferric cytochrome *c* method in the absence or presence of the inhibitors KCN (3 mM) and H_2O_2 (5 mM). These concentrations of KCN and H_2O_2 inhibit CuZnSOD and CuZnSOD + FeSOD, respectively. Control samples to measure total SOD activity contained 10 μM KCN to inhibit cytochrome oxidase, but not CuZnSOD. The MnSOD, FeSOD and CuZnSOD isoforms were also resolved on 15% acrylamide native gels using the nitroblue tetrazolium method by incubation or not with inhibitors (Beauchamp & Fridovich, 1971).

APX was extracted with 50 mM potassium phosphate buffer (pH 7.0), 0.5% PVP-10 and 5 mM ascorbate, and its activity was measured by following ascorbate oxidation at 290 nm for 2 min (Asada, 1984). GR was extracted with 50 mM potassium phosphate buffer (pH 7.8), 1% PVP-10, 0.2 mM EDTA and 0.1% Triton X-100, and its activity was measured by following NADPH oxidation at 340 nm for 3 min (Dalton *et al.*, 1986). MR and DR were extracted with the same medium as for GR but omitting Triton X-100 and including 10 mM

β-mercaptoethanol. MR activity was determined by following NADH oxidation at 340 mm for 90 s (Dalton *et al.*, 1993) and DR activity by following ascorbate formation at 265 nm for 3 min (Nakano & Asada, 1981).

Ascorbate was quantified by MS as indicated below for other organic acids. Glutathione and homoglutathione were quantified by HPLC with fluorescence detection after thiol derivatization with monobromobimane, and the redox state of homoglutathione was determined by an enzymatic recycling method (Matamoros *et al.*, 1999).

Immunoblots

Proteins were extracted from roots at 0°C with 50 mM potassium phosphate buffer (pH 7.8), 0.1% Triton X-100 and 0.1 mM EDTA. Proteins were separated on 12.5% sodium dodecylsulfate gels (Bio-Rad), transferred onto polyvinylidene fluoride membranes and challenged with optimal concentrations of polyclonal antibodies raised against cytosolic DR (DRc) of rice (*Oryza sativa*; Eltayeb *et al.*, 2006), plastidic CuZnSOD (CuZnSODp) of *Spinacia oleracea* (Kanematsu & Asada, 1990) and cytosolic FeSOD (FeSODc) of *Vigna unguiculata* (Moran *et al.*, 2003). The antibody for CuZnSODp also recognizes cytosolic CuZnSOD (CuZnSODc), but both proteins are clearly separated on immunoblots. The secondary antibody for DRc was anti-guinea pig immunoglobulin G conjugated to horseradish peroxidase (Sigma-Aldrich), and was used at a dilution of 1 : 10 000. The secondary antibody for CuZnSODp and FeSODc was anti-rabbit immunoglobulin G conjugated to horseradish peroxidase, and was used at dilutions of 1 : 2000 and 1 : 10 000, respectively. Immunoreactive proteins were visualized using the Supersignal West Pico (Pierce, Rockford, IL, USA) chemiluminescent reagent for peroxidase detection.

Organic acids

Organic acids were analyzed as described elsewhere (Rellán-Álvarez *et al.*, 2011). Briefly, 100 mg of roots were extracted with 2 ml of 4% metaphosphoric acid, 1% PVP-10 and 0.1% formic acid. Samples were centrifuged, filtered and analyzed with a micrOTOF II electrospray ionization mass spectrometer (Bruker Daltonics, Bremen, Germany) coupled to an Alliance 2795 HPLC system (Waters, Milford, MA, USA). Samples were separated isocratically on a Supelcogel H (250 × 4.6 mm, 9 μm; Supelco, Bellefonte, PA, USA) anion exchange column. Internal standards (100 μM of ^{13}C-labeled malic or succinic acids) were used for quantification.

Metabolite profiling

Frozen roots were ground in microvials with stainless steel metal balls using a ball mill grinder, taking care that all material had been precooled with liquid nitrogen. Metabolites were extracted from the frozen powder (60 mg) with methanol/chloroform, and the polar fraction was prepared by liquid partitioning into water and derivatized (Desbrosses *et al.*, 2005). Gas chromatography

coupled to electron impact ionization/time-of-flight (TOF) MS was performed using an Agilent (Santa Clara, CA, USA) 6890N24 gas chromatograph with split or splitless injection connected to a Pegasus III TOF mass spectrometer (LECO, St Joseph, MI, USA) as described by Sánchez *et al.* (2008). Details of the procedures followed for metabolite identification, normalization and quantification have been described previously (Desbrosses *et al.*, 2005; Sánchez *et al.*, 2008).

Proteomic profiling

Proteomic analyses were performed using a gel-free shotgun protocol based on nano-HPLC and MS/MS, as described elsewhere (Larrainzar *et al.*, 2007). In brief, proteins were extracted from roots by acetone precipitation and subjected to in-solution digestion with endoproteinase Lys-C and immobilized trypsin beads. The resulting peptides were desalted, dried and dissolved in formic acid. Protein digests were separated with an Ultra HPLC Eksigent system (Axel Semrau, Sprockhövel, Germany) using a monolithic reversed phase column (Chromolith 150 × 0.1 mm; Merck, Darmstadt, Germany) directly coupled to an Orbitrap XL mass spectrometer (Thermo Scientific, Rockford, IL, USA). Peptides were eluted with a 100-min gradient from 5% to 60% acetonitrile. Dynamic exclusion settings were as described in Hoehenwarter & Wienkoop (2010). After MS analysis, raw files were searched against the DFCI Lotus Gene Index (6.0) using the Sequest algorithm. For identification and spectral count-based data matrix generation, the Proteome Discoverer (v 1.1, Thermo Scientific) was used. A decoy database enabled false positive rate analysis. Only high confidence peptides (false positive rate < 0.1%) with better than 5 ppm precursor mass accuracy and at least two distinct peptides per protein passed criteria.

Results

Plant growth and nutrition

The inhibition of root growth is a typical symptom of Al toxicity (Kochian, 2005) and was used here as a marker to set up treatment conditions of *L. corniculatus* plants grown in hydroponic cultures. We used simple salt solutions to minimize problems with Al speciation and precipitation (Pellet *et al.*, 1995), and selected two low Al concentrations (10 and 20 μM, equivalent to 6.5 and 13 μM of free Al^{3+} activity, respectively) and a period of treatment (14 d) long enough to allow for physiologically relevant changes in growth parameters and in the metabolome and proteome of roots. Plants grown in simple salt solution did not show symptoms of nutrient deficiency and were also comparable in size (Fig. S1c). This was confirmed by the similar contents of N in the roots (22 mg g^{-1} dry weight (DW)) and leaves (28 mg g^{-1} DW) of plants grown in $CaCl_2$ at pH 4.0 with respect to those found in plants grown in 1 : 4 strength B&D solution at pH 4.0 (Broughton & Dilworth, 1971). By contrast, plant treatment with 10 or 20 μM Al increased the N content of roots by *c.* 20% (Supporting Information Table S1) and decreased that of leaves by *c.* 44% (data not shown), which is probably reflective of
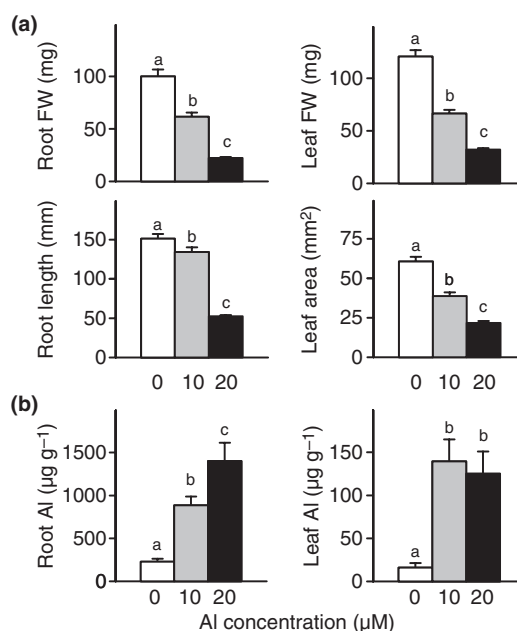

Fig. 1 Effect of aluminum (Al) concentration on growth parameters (a) and the Al contents of roots and leaves (b) of *Lotus corniculatus*. Values are means ± SE of 40–100 replicates, and those denoted by the same letter are not significantly different at *P* < 0.05 according to Duncan's multiple range test. The water contents of roots and leaves of control and Al-treated plants were 91 ± 1% and 82 ± 1%, respectively.

a differential effect of Al on N assimilation in the two plant organs and/or changes in N allocation between root and shoot. Treatment with 20 μM Al caused significant decreases in K, S, Zn and Ni in the roots (Table S1), but no changes in Ca, Mg, P, Fe, Cu and Mn (data not shown).

Plants supplied with 10 μM Al showed a reduction of 11% in the root length and 39% in the root FW (Fig. 1a). The corresponding decreases with 20 μM Al were 52% and 78%. The shoot growth was also affected by application of 10 and 20 μM Al, with decreases of 45% and 73% in FW and of 36% and 64% in leaf area, respectively (Fig. 1a). These plants accumulated Al in the roots and, albeit at 10-fold lower levels, in the leaves (Fig. 1b).

ROS, antioxidant defenses and oxidative damage

Specific fluorescent probes were used to localize Al accumulation and to detect ROS production in roots (Fig. 2). The localization of Al was demonstrated using morin, which strongly binds Al forming a complex that emits green fluorescence. Roots treated with 10 μM Al accumulated this metal along the root, but especially at the tips, which include the cell division and elongation zones. A similar distribution was observed for roots treated with 20 μM Al, although, in this case, fluorescence was more intense. Superoxide radical production was visualized using a method based on the superoxide-mediated oxidation of DHE to oxyethidium, which emits red fluorescence. A low background signal was observed in roots treated with 0 or 10 μM Al, whereas intense red fluorescence was found in roots treated with 20 μM Al, especially at the tips. The production of H_2O_2 and other hydroperoxides was visualized after intracellular oxidation of
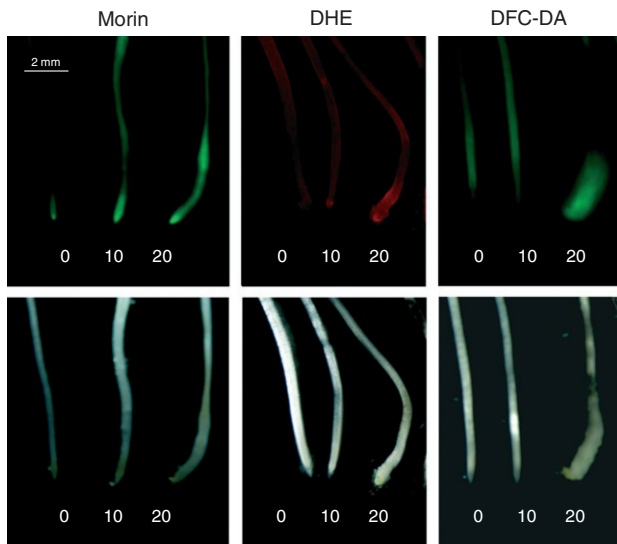
Fig. 2 Localization of aluminum (Al) accumulation using morin and the detection of superoxide radical and peroxide production employing the fluorescent probes dihydroethidium (DHE) and 2′,7′-dichlorofluorescein diacetate (DCF-DA), respectively, in roots of *Lotus corniculatus* exposed to 0 (control), 10 or 20 μM Al. The top images correspond to roots viewed with fluorescence excitation, and the bottom images to the same roots examined with white light to mark the position of the roots. Representative images of at least four independent experiments are shown and the size bar is identical for all panels. Note the deformation of the root tip in plants treated with 20 μM Al.

DCF-DA to a derivative that emits green fluorescence. As was the case for superoxide formation, a strong fluorescence signal was clearly seen in the tips of roots treated with 20 μM Al.

Because plant treatment with the higher Al concentration elicited ROS production and may potentially give rise to oxidative stress, we examined the effects of Al on the expression of key antioxidant enzymes in the roots (Fig. 3). The addition of 10 or 20 μM Al to the rooting medium increased the mRNA level of FeSODc and decreased that of plastidic FeSOD (FeSODp). Moreover, 20 μM Al downregulated the expression of CuZn-SODc, GPX1, GPX4, DRc and plastidic DR (DRp). Neither of the two Al concentrations altered significantly the mRNA levels of MnSOD and other GPXs or those of the APX, MR and GR isoforms (Fig. 3). Likewise, the activities of these three enzymes of the ascorbate–glutathione pathway remained unaffected by Al stress (data not shown).

We further investigated whether the changes in the mRNA levels of the cytosolic enzymes, namely CuZnSODc, FeSODc and DRc, were reflected in the protein contents and enzyme activities of root extracts using immunoblots and activity assays (Fig. 4). The downregulation of *CuZnSODc* and the upregulation of *FeSODc* were accompanied by similar trends in the proteins and catalytic activities. Interestingly, the total SOD and MnSOD activities of the roots remained constant with Al (data not shown), implying a compensation between the CuZnSODc and FeSODc activities. Likewise, the downregulation of the *DRc* gene with Al was paralleled by a marked decrease in protein and activity. Although the DR activity assay could not distinguish between the cytosolic and plastidic isoforms, we found, using a
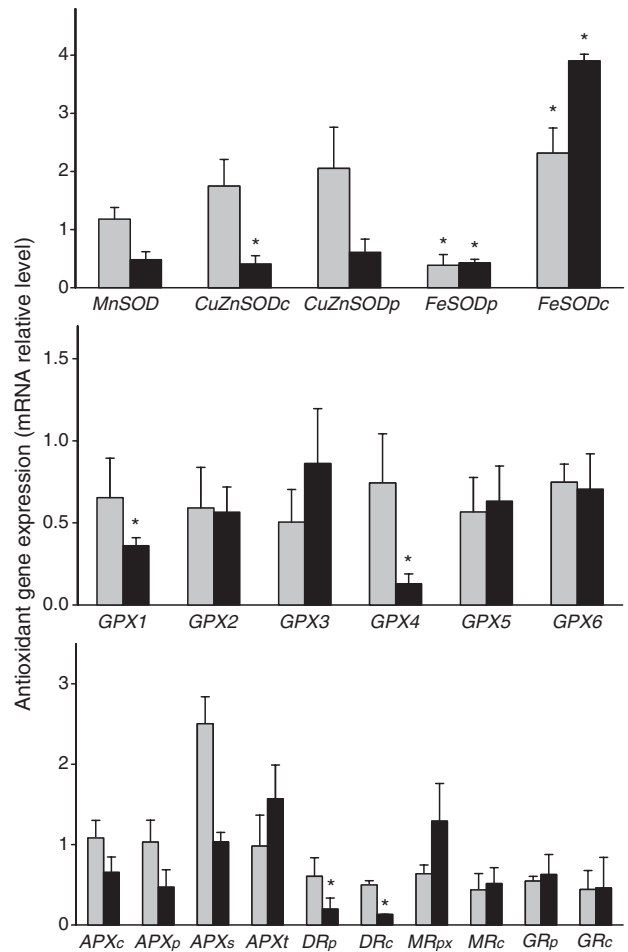

Fig. 3 Expression of antioxidant genes (steady-state mRNA levels) in roots of *Lotus corniculatus* exposed to 10 (gray bars) or 20 (black bars) μM Al. Data of Al-treated plants are expressed relative to those of control plants, which were given a value of unity, and represent the means ± SE of six biological replicates (RNA extractions) from at least two series of plants grown independently. Asterisks denote significant upregulation ($R > 2$) or downregulation ($R < 0.5$) of the genes. APX, ascorbate peroxidase; c, cytosolic isoform; DR, dehydroascorbate reductase; GPX, glutathione peroxidase; GR, glutathione reductase; MR, monodehydroascorbate reductase; p, plastidic isoform; px, peroxisomal isoform; s, stromal isoform; SOD, superoxide dismutase; t, thylakoidal isoform.

specific antibody, that the DRp protein was virtually undetectable in root extracts, and hence the majority of DR activity can be attributed to DRc.

The effects of Al on the major antioxidant metabolites and on lipid peroxidation were also investigated. However, our first attempts to quantify ascorbate using the ascorbate oxidase method failed, probably because traces of Al in the root extracts interfered with the activity assay. Thus, we had to resort to a highly sensitive HPLC-MS method, which allowed us to quantify ascorbate, but not dehydroascorbate. This oxidized form of ascorbate is broken down during the electrospray process, even at the low voltages used here for organic acid analysis (Rellán-Álvarez *et al.*, 2011). The ascorbate content of roots declined by 25% and 55% with 10 and 20 μM Al, respectively (Fig. 5a). The thiol tripeptides glutathione (γGlu-Cys-Gly) and homoglutathione
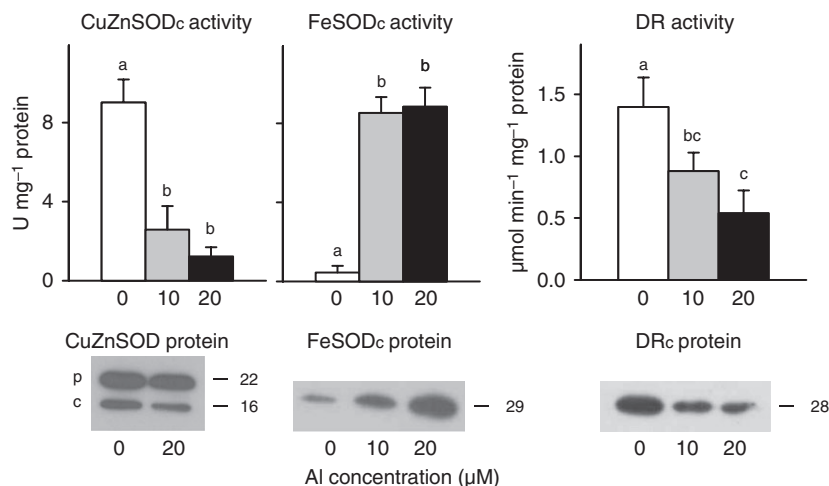
Fig. 4 Specific activities and relative protein abundance of the CuZnSODc, FeSODc and DRc isoforms in roots of *Lotus corniculatus* exposed to 0 (control), 10 or 20 μM Al. Enzyme activities are means ± SE of six replicates, each corresponding to a different root of two series of plants grown independently. Means denoted by the same letter are not significantly different at $P < 0.05$ according to Duncan's multiple range test. Immunoblots are representative of four independent experiments and the apparent molecular masses (kDa) of the proteins are indicated on the right. Lanes were loaded with 20 μg (CuZn-SOD) or 30 μg (FeSODc and DRc) of protein. c, cytosolic isoform; DR, dehydroascorbate reductase; p, plastidic isoform; SOD, superoxide dismutase.
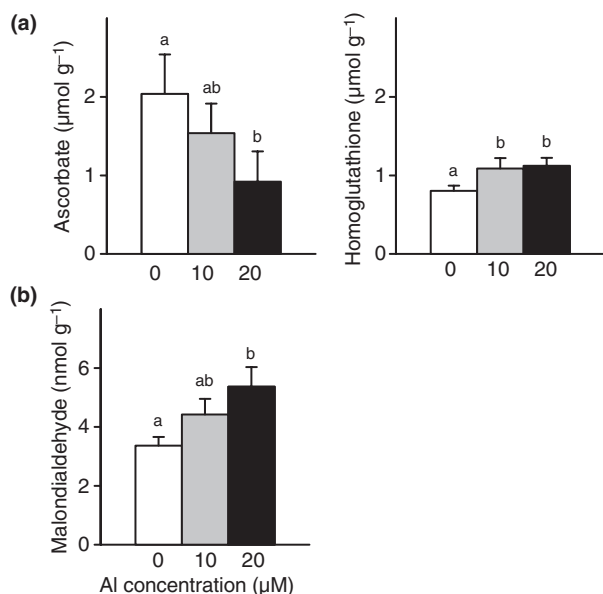

Fig. 5 Contents of antioxidant metabolites (a) and malondialdehyde (b) in roots of *Lotus corniculatus* exposed to 0 (control), 10 or 20 μM Al. Values are means ± SE of 6–12 replicates, each corresponding to a different root of at least two series of plants grown independently. Means denoted by the same letter are not significantly different at $P < 0.05$ according to Duncan's multiple range test.

(γGlu-Cys-βAla) were also quantified in roots. Homoglutathione is only found in certain legume species and tissues, whereas glutathione is ubiquitous in plants and other organisms (Matamoros *et al.*, 1999). The roots and leaves of *L. corniculatus* contained 3% glutathione and 97% homoglutathione. The content of total homoglutathione (reduced + oxidized forms) in roots increased by *c.* 35% with 10 or 20 μM Al (Fig. 5a). However, the redox state of homoglutathione (percentage of the reduced form) remained in the range 88–90% for both Al treatments. The

oxidative damage of lipids was used as a marker of oxidative stress and assessed by measuring malondialdehyde, a decomposition product of lipid peroxides. The content of malondialdehyde in roots did not change with 10 μM Al, but increased significantly with 20 μM Al (Fig. 5b).

Organic acids and metabolomics

The organic acids most commonly found in plant cells were quantified in roots by HPLC-MS, as some of these compounds constitute a defense mechanism against Al toxicity and their concentrations may be responsive to Al (Pellet *et al.*, 1995; Ma *et al.*, 2001). Moreover, a metabolomic approach was used to study the possible effects of Al on other metabolic pathways in the roots. Both types of analysis were also carried out in the leaves to determine whether the low amounts of Al detected in the shoot interfered with leaf metabolism. Plant treatment with 10 and/or 20 μM Al caused an increase in malate, succinate and fumarate, a decrease in citramalate and no changes in citrate in the roots (Fig. 6). However, the concentrations of these carboxylic acids remained unaffected in the leaves (data not shown).

Metabolite profiling of roots and leaves of Al-treated plants revealed changes in important amino acids and sugars, as well as in certain organic acids that had not been analyzed by HPLC-MS (Table 1). In roots and leaves, there was an important increase in the asparagine content. This amino acid is a major product of ammonium assimilation in *L. corniculatus* roots. In addition, Al treatment caused a decline in the root content of glycine and increases in the leaf contents of serine, aspartic acid and glutamic acid, indicating that Al also affected amino acid metabolism and/or protein turnover in the shoot. Likewise, Al stress increased the concentrations of five carboxylic acids in the roots. These included two malic acid derivatives and threonic acid, a product of ascorbic acid metabolism. The largest increases, in the range 80–100%, were found for threonic, 2-isopropylmalic and
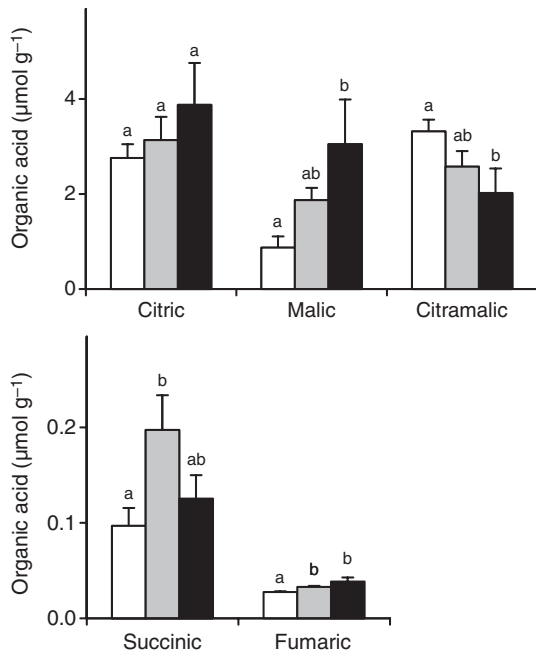
Fig. 6 Contents of several carboxylic acids in roots of *Lotus corniculatus* exposed to 0 (control; white bars), 10 (gray bars) or 20 (black bars) μM Al. Values are means ± SE of nine replicates, each corresponding to a different root of three series of plants grown independently. Means denoted by the same letter are not significantly different at $P < 0.05$ according to Duncan's multiple range test.

Table 1 Effects of aluminum (Al) stress on the metabolite contents of roots and leaves of *Lotus corniculatus*

	Al concentration (μM)		
Roots	0	10	20
Amino acids			
Asparagine	8.7 ± 0.7 a	10.9 ± 1.3 ab	13.1 ± 0.8 b
Glycine	1.0 ± 0.1 a	0.5 ± 0.0 b	0.7 ± 0.1 a
Organic acids			
Threonic acid	3.8 ± 0.4 a	6.8 ± 0.4 b	6.8 ± 0.8 b
2-Isopropylmalic acid	5.1 ± 1.0 a	5.5 ± 0.8 a	10.1 ± 0.6 b
2-Methylmalic acid	8.2 ± 0.8 ab	6.4 ± 0.8 a	9.7 ± 0.7 b
Pyroglutamic acid	9.7 ± 0.7 ab	8.1 ± 0.3 a	10.0 ± 0.3 b
Glyceric acid	0.6 ± 0.1 a	0.8 ± 0.0 a	1.1 ± 0.1 b
Sugars			
Glucose	9.9 ± 0.9 a	14.4 ± 1.3 b	9.3 ± 0.9 a
Fructose	10.9 ± 0.7 a	14.4 ± 1.1 b	9.4 ± 1.0 a
Sucrose	18.7 ± 0.9 a	14.6 ± 0.4 b	17.4 ± 0.5 a
Sedoheptulose	10.6 ± 0.9 a	11.6 ± 1.5 a	7.6 ± 1.1 b
Polyols			
Pinitol	9.9 ± 0.6 ab	8.8 ± 0.2 a	10.8 ± 0.3 b
Leaves	0	10	20
Amino acids			
Serine	12.1 ± 0.9 a	18.2 ± 1.6 b	14.3 ± 0.9 ab
Asparagine	0.5 ± 0.1 a	3.2 ± 1.0 b	1.0 ± 0.1 b
Aspartic acid	1.5 ± 0.3 a	4.2 ± 0.9 b	3.2 ± 0.5 b
Glutamic acid	8.3 ± 0.5 a	12.9 ± 1.0 b	13.6 ± 0.6 b
Organic acids			
Succinic acid	8.6 ± 0.7 a	10.7 ± 0.7 a	13.9 ± 0.6 b
Threonic acid	7.9 ± 0.5 a	11.6 ± 1.1 b	14.0 ± 0.5 b
Threonic acid-1,4-lactone	11.6 ± 0.9 a	13.8 ± 1.0 ab	14.7 ± 0.8 b
Galactonic acid	13.0 ± 0.2 a	14.1 ± 0.6 a	16.3 ± 0.6 b
2-Isopropylmalic acid	8.2 ± 1.4 a	14.2 ± 1.9 b	13.2 ± 1.6 ab
Sugars			
Glucose	7.9 ± 0.6 a	8.4 ± 0.8 a	12.2 ± 1.1 b
Fructose	7.7 ± 0.7 a	7.8 ± 0.7 a	11.1 ± 1.1 b
Sucrose	13.1 ± 0.4 a	13.9 ± 0.4 a	16.0 ± 0.5 b
Polyols			
Pinitol	24.0 ± 1.7 a	19.2 ± 0.9 b	20.1 ± 0.7 ab

Values represent normalized responses of metabolite pool measurements (detector signals in arbitrary units normalized to internal standard and sample fresh weight). Data are means ± SE of 12 biological replicates from two series of plants grown independently. Means denoted by the same letter are not significantly different at $P < 0.05$ according to Duncan's multiple range test.

glyceric acids. The concentrations of threonic and 2-isopropylmalic acids were also augmented by *c.* 70% in the leaves of plants treated with 10 or 20 μM Al. These plants also showed alterations in the sugar concentrations of roots and leaves. Thus, in roots treated with 10 μM Al, glucose and fructose increased concomitant with a modest decline in sucrose, whereas, in the leaves, glucose, fructose and sucrose remained constant with 10 μM Al, but increased by 22–54% with 20 μM Al (Table 1).

Proteomics

A highly sensitive analysis of the root proteome, entailing nano-HPLC shotgun MS, allowed us to identify proteins that were newly induced or upregulated, as well as those that were suppressed or downregulated, in response to Al stress (Table 2). Proteins were identified based on the sequences available in the *L. japonicus* databases and were classified into functional groups. For relative quantification, the spectral count number was used as described by Larrainzar *et al.* (2007). An independent component analysis of the data revealed a progressive separation of the Al-treated samples relative to control samples with increasing Al concentration (Fig. S2). Particularly critical for this separation were the loadings of the first independent component, which accounted for 50% of the total variance.

The treatment of plants with 10 and/or 20 μM Al led to major decreases in the root contents of proteins implicated in multiple crucial processes, such as cell elongation and division, protein synthesis and degradation, amino acid and organic acid metabolism, glycolysis and carbohydrate metabolism, transport, redox control and stress response (Table 2). Some of these proteins were already undetectable in roots exposed to only 10 μM Al, whereas others were suppressed after application of 20 μM Al. The first group included a β-tubulin chain, pyruvate kinase, ferredoxin-NADP reductase and caffeoyl-CoA *O*-methyltransferase; the second group included some β-tubulin and ribosomal polypeptides, histones, UTP-glucose-1-P uridyltransferase, phosphoglycerate dehydrogenase, protein disulfide isomerase, a peroxidase precursor and a lipoxygenase isoform. In sharp contrast, a few proteins were newly induced with 10 μM Al and their levels were further enhanced with 20 μM Al. This was the case for the proteasome α-subunit and two peroxidase isoforms. Finally, the contents of other proteins that were constitutively expressed in

Table 2 Effects of aluminum (Al) stress on the *Lotus corniculatus* root proteome

Protein	TC[1]	UniProt[2]	Al concentration (μM)		
			0	10	20
Cell wall/cell organization					
α-Tubulin	TC62930	A9PL19	1129 a	877 a	181 b
α-Tubulin	TC63835	Q2TFP2	897 a	718 a	140 b
β-Tubulin	TC61113	UPI00015CD56A	699 a	0 b	0 b
β-Tubulin	TC63392	P29514	1067 a	556 b	0 c
β-Tubulin	TC62547	P37392	1081 a	570 b	0 c
β-Tubulin	TC57323	Q40665	1073 a	556 b	0 c
Gene structure and regulation					
Histone H2A	BW599450	A7P108	347 a	50 ab	0 b
Histone H2A	TC61686	A2WQG7	656 a	116 b	0 b
Histone H4	TC70944	UPI000050340F	556 a	351 a	0 b
Protein synthesis					
60S ribosomal protein	BW604002	Q8H2B9	381 a	80 b	0 b
60S ribosomal protein L9	FS326259	P30707	754 a	317 b	0 c
Elongation factor 1-α	TC69520	Q3LUM5	1043 a	786 a	140 b
Elongation factor 1-α	TC73117	Q3LUM2	1467 a	1204 ab	701 b
Elongation factor 1-β	FS339508	P29545	892 a	734 a	191 b
Elongation factor 1-γ	TC60762	Q8S3W1	708 a	413 ab	120 b
Elongation factor EF-2 (putative)	TC75757	Q9ASR1/Q9SGT4	1394 a	1085 a	311 b
Protein degradation					
Cysteine proteinase inhibitor	BI418502	Q06445	80 a	463 ab	156 b
Proteasome subunit α type	TC57402	A7P6B1	0 a	116 b	426 b
Peptidase C1A	TC68381	Q2HTQ3	296 a	660 a	1146 b
Polyubiquitin	TC81524	A1X1E5	0 a	50 a	410 b
Polyubiquitin	TC81113	Q0J9W6	0 a	50 a	457 b
Transport					
Adenine nucleotide translocator (mitochondrial)	TC74603	O49875	392 a	426 a	0 b
ATP synthase subunit γ (mitochondrial)	TC57922	D7SI12	310 a	50 ab	0 b
ATP synthase catalytic subunit A (vacuolar)	TC75345	Q9SM09	959 a	877 a	295 b
Amino acid metabolism					
Methionine synthase	TC70396	Q71EW8	1411 a	1157 a	402 b
Methionine synthase	TC65903	UPI00015CD060	793 a	698 a	0 b
S-Adenosylmethionine synthetase	TC69893	A4PU48	1358 a	1262 ab	874 b
S-Adenosylmethionine synthetase	TC67258	A4ULF8	1311 a	1257 a	816 b
Adenosylhomocysteinase 1	TC72761	O23255	925 a	910 a	169 b
Glutamine synthetase (cytosolic isoform)	TC72874	Q42899	1490 a	1287 a	753 b
Organic acid metabolism					
Malate dehydrogenase	TC62158	Q9SPB8	1250 a	963 a	208 b
Malate dehydrogenase	TC66662	Q6RIB6	1181 a	985 ab	499 b
Malate dehydrogenase	TC59388	O81278	580 a	217 b	0 b
Isocitrate dehydrogenase	TC67164	Q06197	910 a	794 ab	426 b
Carbonic anhydrase	TC57320	Q5NE21	1069 a	587 b	95 c
Carbohydrate metabolism					
UTP-Glucose-1-P uridylyltransferase	TC59881	Q9LKG7	506 a	280 ab	0 b
Sucrose synthase	TC77381	P13708	965 a	658 a	169 b
Sucrose synthase	TC72460	Q9AVR8	823 a	453 ab	120 b
Sucrose synthase (nodule enhanced)	TC78224	O81610	1111 a	879 ab	435 b
Fructokinase-2 (putative)	TC74169	Q9LNE3	1383 a	1084 ab	605 b
UDP-Glucose:protein transglucosylase-like	TC76160	Q38M71	1101 a	835 ab	429 b
Glycolysis					
Pyruvate kinase	TC58669	Q5F2M7	429 a	0 b	0 b
Phosphoglycerate kinase	TC78075	A5CAF8	734 a	522 ab	156 b
Phosphoglycerate kinase	TC57762	Q9LKJ2	1170 a	962 ab	467 b
Phosphoglycerate dehydrogenase (putative)	TC65829	UPI00015C90B8	246 ab	547 a	0 b
Enolase	TC58226	Q6RIB7	1093 a	870 a	309 b
Electron transfer/redox/antioxidant					
Ferredoxin-NADP reductase	TC60743	Q41014	400 a	0 b	0 b
Catalase	TC58073	A0PG70	597 a	310 ab	140 b
Pox09	TC57306	Q9XFL3	0 a	180 b	311 b
Pox13 (precursor)	TC60841	Q9ZNZ6	749 a	310 b	0 b
Pox30	TC61834	A4UN76	0 a	852 b	1054 b

Table 2 (Continued)

Protein	TC[1]	UniProt[2]	Al concentration (μM)		
			0	10	20
GST15 (tau class)	TC57307	Q9FQE3	151 a	239 ab	536 b
GSTin2-1 (lambda class)	TC57627	Q9FQ95	50 a	251 a	854 b
Protein disulfide-isomerase A6 precursor (putative)	TC72404	P38661	259 a	80 ab	0 b
Lipoxygenase	TC57788	O24470	180 ab	458 a	0 b
Stress					
Heat shock protein 70	GO008419	Q40980	1179 a	906 ab	511 b
Heat shock cognate protein 70	TC58352	Q40151	1135 a	1087 a	703 b
Heat shock cognate protein 70	TC77297	Q5QHT3	1189 a	940 ab	587 b
Heat shock cognate protein 70	TC68669	Q41027	1302 a	1140 ab	760 b
Heat shock protein 90	TC60546	A8WEL7	909 a	722 a	169 b
BiP-isoform D	TC73211	Q9ATB8	1110 a	893 ab	501 b
PR protein class 10	TC57863	Q94IM3	680 a	1221 b	1188 b
Secondary metabolism					
Caffeoyl-CoA O-methyltransferase	TC58984	Q40313	467 a	0 b	0 b

Values ((log of the number of spectral counts) × 1000) are means of six biological replicates from two series of plants grown independently. Means denoted by the same letter are not significantly different at $P < 0.05$ according to Duncan's multiple range test.
[1]Tentative consensus (TC) sequence numbers according to the DFCI Lotus Gene Index (6.0).
[2]UniProt accessions (UniRef100).

roots increased in response to Al. Notable examples of this were the cysteine proteinase inhibitor and peptidase C1A, two glutathione transferases (formerly glutathione S-transferases; GSTs) and a pathogenesis-related class 10 (PR-10) protein (Table 2).

The identification of peroxidases and GSTs responsive to Al is presented separately in further detail in Table S2, given the bewildering complexity of these two groups of enzymes that perform multiple roles in plants in addition to those related to their antioxidative properties. There are between 70 and 100 class III or secretory peroxidases (deposited in the PeroxiBase; see Table S2; Cosio & Dunand, 2009) and between 25 and 54 GSTs (McGonigle et al., 2000; Dalton et al., 2009; Dixon et al., 2010) in legumes and other plants. However, only three peroxidases (Pox09, Pox13 and Pox30) and two GSTs (GST15 and GSTin2-1) were affected at the protein level in *L. corniculatus* roots exposed to Al stress (Table 2).

Discussion

In this work, *L. corniculatus* plants were exposed to low Al concentrations for a prolonged time to mimic the acidic soil conditions prevailing in some regions of South America, where this forage legume is amply cultivated. In Uruguay, 1 080 000 hectares are sown in mixed legume–grass pastures and 117 000 hectares in pure pastures (DIEA, 2010). In preliminary experiments, two Al concentrations were carefully selected in an attempt to discriminate between the toxic effects of Al and oxidative stress. The long-term application of 10 μM Al to *L. corniculatus* plants was sufficient to inhibit markedly root and shoot growth. At this stage, there was accumulation of Al, but not of ROS, in the root tip. Moreover, the mRNA levels and activities of antioxidant enzymes, with few exceptions, and the malondialdehyde content were not affected. By contrast, increasing the Al concentration from 10 to 20 μM induced oxidative stress in the roots. The accumulation of malondialdehyde with 20 μM Al can be explained by

an exacerbated production of superoxide and H_2O_2, which may give rise, in the presence of catalytic metal ions, to hydroxyl radicals and other highly oxidizing species necessary to initiate membrane fatty acid peroxidation (Halliwell & Gutteridge, 2007). Other authors have found, using different experimental conditions, an increase in lipid peroxidation in plants treated with Al (Cakmak & Horst, 1991; Yamamoto et al., 2001; Guo et al., 2004; Sharma & Dubey, 2007).

The decrease in ascorbate, which is required for α-tocopherol regeneration, may also contribute to the cumulative peroxidative damage in *L. corniculatus* roots. Notably, DRc activity, which reduces dehydroascorbate to ascorbate, was transcriptionally downregulated. Dehydroascorbate is quite unstable and, unless rapidly used up by DRc to regenerate ascorbate, is degraded to oxalate and threonate (Green & Fry, 2005). The downregulation of DRc may thus explain the decrease in ascorbate concurrent with the accumulation of threonate in Al-treated roots. Another novel finding related to antioxidant protection was the progressive replacement of CuZnSODc by FeSODc with Al stress. This may be explained by a microRNA-mediated cleavage of the *CuZnSODc* mRNA. Thus, in *A. thaliana* plants under low Cu conditions, the *miR398* family is involved in the downregulation of CuZnSODc and CuZnSODp, which are replaced by FeSOD (Yamasaki et al., 2007). In *L. corniculatus* roots, the total contents of Cu or Zn (mainly as constituents of metalloproteins) remained unchanged or decreased with Al, respectively. We cannot rule out the possibility that a lower availability of free Cu^{2+} and/or Zn^{2+} ions downregulates the synthesis of functional CuZnSOD in Al-treated plants. Interestingly, the so-called 'cytosolic' CuZnSOD and FeSOD isoforms are also present, and at relatively large amounts, in the nuclei (Rubio et al., 2009). We found no apparent functional reason for the change in the prevalent SOD isoform in the cytosol and nuclei of root cells stressed by Al because both types of enzyme are potentially inactivated by H_2O_2. In any case, this 'switch' of SOD isoform seems to be associated with

advancing senescence, at least in legume nodules (Moran *et al.*, 2003; Rubio *et al.*, 2007), indicating a compensatory phenomenon between the two enzyme activities.

The combined use of organic acid analysis, metabolomics and proteomics allowed us to unravel some cellular functions and metabolic pathways responsive to Al stress in *L. corniculatus*. One such pathway is dicarboxylic acid metabolism. Roots exposed to Al have higher concentrations of malic, succinic and fumaric acids. This alteration may be related to the decrease in cytosolic malate dehydrogenase and isocitrate dehydrogenase, observed in our proteomic study, rather than to a specific effect on the citric acid cycle in mitochondria. A detrimental effect of Al on the cytosol of root cells is also substantiated by the strong downregulation of key enzymes involved in sucrose metabolism and glycolysis, as well as by the changes in DRc, CuZnSODc and FeSODc proteins and activities mentioned above. Metabolite profiling led us to identify lesser known organic acids that are also affected by Al stress. Thus, the content of 2-isopropylmalic acid, an intermediate in leucine biosynthesis, increased in roots and leaves. This compound is secreted by budding yeast (*Saccharomyces cerevisiae*) cells challenged with Al (Kobayashi *et al.*, 2005), and may be involved in its detoxification as it is a powerful chelator of Al^{3+} (Tashiro *et al.*, 2006). Although the identification of organic acids secreted by *L. corniculatus* roots is beyond the scope of this study, our results are consistent with a role of malate and 2-isopropylmalate, rather than citrate, in Al detoxification. Thus, in addition to the changes in the root contents of both dicarboxylates and their associated enzymes, we found increases of 5.5-fold with 10 μM Al and nine-fold with 20 μM Al in the *ALMT* mRNA levels (Fig. S3).

Plant treatment with Al had major effects on cytoskeleton dynamics and protein turnover in the roots. Exposure to 10 and/or 20 μM Al drastically reduced the amounts of α- and β-tubulin and of some ribosomal proteins and elongation factors. These changes are consistent with an inhibitory effect of Al on cell division and protein synthesis. In particular, the root tips were seriously deformed with 20 μM Al as a result of the inhibition of root cell elongation and division. This Al concentration stimulated protein degradation, judging from the increase in the root content of proteases and of the 20S proteasome α-subunit. An induction of the latter protein has been observed in Al-treated tomato (*Solanum lycopersicum*) roots (Zhou *et al.*, 2009). The application of 20 μM Al to plants also had a strong impact on methionine metabolism. This amino acid is essential not only as a constituent of proteins, but also as a direct precursor of *S*-adenosylmethionine, which is a major methyl group donor and an intermediate in the biosynthesis of ethylene, polyamines, biotin and nicotianamine (Moffatt & Weretilnyk, 2001; Ravanel *et al.*, 2004). The three enzymes intervening in the activated methyl cycle (methionine synthase, *S*-adenosylmethionine synthetase and *S*-adenosylhomocysteine hydrolase) were strongly downregulated with Al stress. This downregulation may result in a restriction of transmethylation reactions and/or alterations in the biosynthesis of hormones, such as ethylene, in the root cells. Recent work has shown that *S*-adenosylmethionine synthetase and *S*-adenosylhomocysteine hydrolase are moderately induced

by Al in tomato roots (Zhou *et al.*, 2009) and that two *S*-adenosylmethionine synthetase isoforms are differentially regulated in rice roots (Yang *et al.*, 2007). Overall, these results show that the methyl cycle is a preferential target of Al toxicity.

As anticipated, plant treatment with Al elicited changes in redox and stress proteins. Class III peroxidases and GSTs are multifunctional enzymes encoded by large gene families. However, the response to Al stress was rather specific, as only two isoforms of each family were induced in *L. corniculatus* roots. To our knowledge, no changes in the content of peroxidase isoforms in Al-treated roots have been reported to date, although the expression of several peroxidase genes was found to be affected at the transcriptional level in *A. thaliana* (Richards *et al.*, 1998; Kumari *et al.*, 2008). The inducibility of the two GST isoforms strongly suggests that they are efficient at using homoglutathione as substrate, because we found that this glutathione homolog accounts for 97% of the total thiol tripeptides in *L. corniculatus* roots. A transcriptomic analysis of *A. thaliana* showed time-dependent changes in the mRNA levels of various GST genes in response to Al (Kumari *et al.*, 2008), whereas proteomic analyses showed that two different GST isoforms were downregulated in soybean (*Glycine max*; Zhen *et al.*, 2007) and tomato (Zhou *et al.*, 2009). Molecular chaperones play important roles in preventing aggregation and assisting the refolding of non-native proteins, as well as in facilitating proteolytic degradation of unstable proteins (Wang *et al.*, 2004). Interestingly, some heat shock proteins/molecular chaperones of the Hsp70 and Hsp90 families and a protein disulfide isomerase, which may also function as a chaperone, were found to be downregulated. This probably reflects the inability of *L. corniculatus* to withstand 20 μM Al, a conclusion that is supported by the suppression or consistent downregulation of other proteins, not previously reported in proteomic studies, that are involved in gene regulation, transport, electron transfer and hormone synthesis.

In conclusion, under our experimental conditions, 10 μM Al was sufficient to inhibit root and shoot growth and to affect the contents of some metabolites and proteins of root cells, but did not trigger ROS accumulation or oxidative stress. Therefore, oxidative damage was not the cause of Al toxicity. Increasing the Al concentration to 20 μM elicited ROS accumulation and oxidative stress, inhibited protein synthesis, enhanced proteolysis and intensified the effects on the proteins involved in cytoskeleton organization, organic acid and carbohydrate metabolism, redox regulation and stress responses. These detrimental effects indicate a metabolic dysfunction, which affects the cytosol, mitochondria and other cellular compartments, particularly in plants exposed to 20 μM Al. Finally, a practical consequence derived from this work is that attempts to develop tolerance to oxidative stress will not, by themselves, alleviate the problems of Al toxicity.

Acknowledgements

References

Abreu CH Jr, Muraoka T, Lavorante AF. 2003. Relationship between acidity and chemical properties of Brazilian soils. *Scientia Agricola* **60**: 337–343.

Asada K. 1984. Chloroplasts: formation of active oxygen and its scavenging. *Methods in Enzymology* **105**: 422–429.

Barceló J, Poschenrieder C. 2002. Fast root growth responses, root exudates, and internal detoxification as clues to the mechanisms of aluminium toxicity and resistance: a review. *Environmental and Experimental Botany* **48**: 75–92.

Beauchamp C, Fridovich I. 1971. Superoxide dismutase: improved assays and an assay applicable to acrylamide gels. *Analytical Biochemistry* **44**: 276–287.

Boisson-Dernier A, Chabaud M, Garcia F, Bécard G, Rosenberg C, Barker DG. 2001. Hairy roots of *Medicago truncatula* as tools for studying nitrogen-fixing and endomycorrhizal symbioses. *Molecular Plant–Microbe Interactions* **14**: 693–700.

Boscolo PRS, Menossi M, Jorge RA. 2003. Aluminum-induced oxidative stress in maize. *Phytochemistry* **62**: 181–189.

Broughton BJ, Dilworth MJ. 1971. Control of leghaemoglobin synthesis in snake beans. *Biochemical Journal* **125**: 1075–1080.

Cakmak I, Horst WJ. 1991. Effect of aluminium on lipid peroxidation, superoxide dismutase, catalase, and peroxidase activities in root tips of soybean (*Glycine max*). *Physiologia Plantarum* **83**: 463–468.

Cosio C, Dunand C. 2009. Specific functions of individual class III peroxidase genes. *Journal of Experimental Botany* **60**: 391–408.

Czechowski T, Stitt M, Altmann T, Udvardi MK, Scheible WR. 2005. Genome-wide identification and testing of superior reference genes for transcript normalization in Arabidopsis. *Plant Physiology* **139**: 5–17.

Dalton DA, Boniface C, Turner Z, Lindhal A, Kim HJ, Jelinek L, Govindarajulu M, Finger RE, Taylor CG. 2009. Physiological roles of glutathione S-transferases in soybean root nodules. *Plant Physiology* **150**: 521–530.

Dalton DA, Langeberg L, Treneman NC. 1993. Correlations between the ascorbate–glutathione pathway and effectiveness in legume root nodules. *Physiologia Plantarum* **87**: 365–370.

Dalton DA, Russell SA, Hanus FJ, Pascoe GA, Evans HJ. 1986. Enzymatic reactions of ascorbate and glutathione that prevent peroxide damage in soybean root nodules. *Proceedings of the National Academy of Sciences, USA* **83**: 3811–3815.

Darkó E, Ambrus H, Stefanovits-Bányai E, Fodor J, Bakos F, Barnabás B. 2004. Aluminium toxicity, Al tolerance and oxidative stress in an Al-sensitive wheat genotype and in Al-tolerant lines developed by *in vitro* microspore selection. *Plant Science* **166**: 583–591.

Desbrosses GG, Kopka J, Udvardi MK. 2005. *Lotus japonicus* metabolic profiling. Development of gas chromatography-mass spectrometry resources for the study of plant–microbe interactions. *Plant Physiology* **137**: 1302–1318.

Díaz P, Borsani O, Monza J. 2005. *Lotus*-related species and their agronomic importance. In: Márquez AJ, ed. *Lotus japonicus handbook*. Dordrecht, the Netherlands: Springer, 25–37.

DIEA. 2010. *Anuario Estadístico Agropecuario*. Montevideo, Uruguay: Dirección de Estadísticas Agropecuarias. Ministerio de Ganadería, Agricultura y Pesca.

Dixon DP, Skipsey M, Edwards R. 2010. Roles for glutathione transferases in plant secondary metabolism. *Phytochemistry* **71**: 338–350.

Eltayeb AE, Kawano N, Badawi GH, Kaminak H, Sanekatad T, Morishima I, Shibahar T, Inanaga S, Tanaka K. 2006. Enhanced tolerance to ozone and drought stresses in transgenic tobacco overexpressing dehydroascorbate reductase in cytosol. *Physiologia Plantarum* **127**: 57–65.

Eticha D, Zahn M, Bremer M, Yang Z, Rangel AF, Rao IM, Horst WJ. 2010. Transcriptomic analysis reveals differential gene expression in response to aluminium in common bean (*Phaseolus vulgaris*) genotypes. *Annals of Botany* **105**: 1119–1128.

Ezaki B, Gardner RC, Ezaki Y, Matsumoto H. 2000. Expression of aluminum-induced genes in transgenic Arabidopsis plants can ameliorate aluminum stress and/or oxidative stress. *Plant Physiology* **122**: 657–666.

Foyer CH, Noctor G. 2005. Oxidant and antioxidant signalling in plants: a re-evaluation of the concept of oxidative stress in a physiological context. *Plant, Cell & Environment* **28**: 1056–1071.

Green MA, Fry SC. 2005. Vitamin C degradation in plant cells via enzymatic hydrolysis of 4-O-oxalyl-L-threonate. *Nature* **433**: 83–87.

Guo T, Zhang G, Zhou M, Wu F, Chen J. 2004. Effects of aluminum and cadmium toxicity on growth and antioxidant enzyme activities of two barley genotypes with different Al resistance. *Plant and Soil* **258**: 241–248.

Halliwell B, Gutteridge JMC. 2007. *Free radicals in biology and medicine, 4th edn*. Oxford, UK: Oxford University Press.

Handberg K, Stougaard J. 1992. *Lotus japonicus*, an autogamous, diploid legume species for classical and molecular genetics. *Plant Journal* **2**: 487–496.

Hoehenwarter W, Wienkoop S. 2010. Spectral counting robust on high mass accuracy mass spectrometers. *Rapid Communications in Mass Spectrometry* **24**: 3609–3614.

Hoekenga OA, Maron LG, Piñeros MA, Cançado GMA, Shaff J, Kobayashi Y, Ryan PR, Dong B, Delhaize E, Sasaki T et al. 2006. *AtALMT1*, which encodes a malate transporter, is identified as one of several genes critical for aluminum tolerance in *Arabidopsis*. *Proceedings of the National Academy of Sciences, USA* **103**: 9738–9743.

Iturbe-Ormaetxe I, Escuredo PR, Arrese-Igor C, Becana M. 1998. Oxidative damage in pea plants exposed to water deficit or paraquat. *Plant Physiology* **116**: 173–181.

Kanematsu S, Asada K. 1990. Characteristic amino acid sequences of chloroplast and cytosol isozymes of CuZn-superoxide dismutase in spinach, rice and horsetail. *Plant & Cell Physiology* **31**: 99–112.

Kobayashi A, Edo H, Furihata K, Yoshimura E. 2005. Secretion of an aluminum chelator, 2-isopropylmalic acid, by the budding yeast, *Saccharomyces cerevisiae*. *Journal of Inorganic Biochemistry* **99**: 1260–1263.

Kochian LV. 2005. Cellular mechanisms of aluminum toxicity and resistance in plants. *Annual Review in Plant Physiology and Plant Molecular Biology* **46**: 237–260.

Kumari M, Taylor GJ, Deyholos MK. 2008. Transcriptomic responses to aluminum stress in roots of *Arabidopsis thaliana*. *Molecular Genetics & Genomics* **279**: 339–357.

Larrainzar E, Wienkoop S, Weckwerth W, Ladrera R, Arrese-Igor C, González EM. 2007. *Medicago truncatula* root nodule proteome analysis reveals differential plant and bacteroid responses to drought stress. *Plant Physiology* **144**: 1495–1507.

Ma JF, Ryan PR, Delhaize E. 2001. Aluminium tolerance in plants and the complexing role of organic acids. *Trends in Plant Science* **6**: 273–278.

Maron LG, Kirst M, Mao C, Milner MJ, Menossi M, Kochian LV. 2008. Transcriptional profiling of aluminum toxicity and tolerance responses in maize roots. *New Phytologist* **179**: 116–128.

Matamoros MA, Moran JF, Iturbe-Ormaetxe I, Rubio MC, Becana M. 1999. Glutathione and homoglutathione synthesis in legume root nodules. *Plant Physiology* **121**: 879–888.

McGonigle B, Keeler SJ, Lau S-MC, Koeppe MK, O'Keefe DP. 2000. A genomics approach to the comprehensive analysis of the glutathione S-transferase gene family in soybean and maize. *Plant Physiology* **124**: 1105–1120.

Moffatt BA, Weretilnyk EA. 2001. Sustaining S-adenosyl-L-methionine-dependent methyltransferase activity in plant cells. *Physiologia Plantarum* **113**: 435–442.

Moran JF, James EK, Rubio MC, Sarath G, Klucas RV, Becana M. 2003. Functional characterization and expression of a cytosolic iron-superoxide dismutase from cowpea root nodules. *Plant Physiology* 133: 773–782.

Mossor-Pietraszewska T. 2001. Effect of aluminium on plant growth and metabolism. *Acta Biochimica Polonica* 48: 673–686.

Nakano Y, Asada K. 1981. Hydrogen peroxide is scavenged by ascorbate-specific peroxidase in spinach chloroplasts. *Plant Cell Physiology* 22: 867–880.

Pavlovkin J, Pal'ove-Balang P, Kolarovic L, Zelinová V. 2009. Growth and functional responses of different cultivars of *Lotus corniculatus* to aluminum and low pH stress. *Journal of Plant Physiology* 166: 1479–1487.

Pellet DM, Grunes DL, Kochian LV. 1995. Organic acid exudation as an aluminum-tolerance mechanism in maize (*Zea mays* L.). *Planta* 196: 788–795.

Rao IM, Zeigler RS, Vera R, Sarkarung S. 1993. Selection and breeding for acid-soil tolerance in crops. *BioScience* 43: 454–465.

Ravanel S, Block MA, Rippert P, Jabrin S, Curien G, Rébeillé F, Douce R. 2004. Methionine metabolism in plants. Chloroplasts are autonomous for *de novo* methionine synthesis and can import *S*-adenosylmethionine from the cytosol. *Journal of Biological Chemistry* 279: 22548–22557.

Rellán-Álvarez R, López-Gomollón S, Abadía J, Álvarez-Fernández A. 2011. Development of a new HPLC-ESI-TOFMS method for the determination of low molecular mass organic acids in plant tissue extracts. *Journal of Agricultural and Food Chemistry* 59: 6864–6870.

Richards KD, Schott EJ, Sharma YK, Davis KR, Gardner RC. 1998. Aluminum induces oxidative stress genes in *Arabidopsis thaliana*. *Plant Physiology* 116: 409–418.

Rubio MC, Becana M, Kanematsu S, Ushimaru T, James EK. 2009. Immunolocalization of antioxidant enzymes in high-pressure frozen root and stem nodules of *Sesbania rostrata*. *New Phytologist* 183: 395–407.

Rubio MC, Becana M, Sato S, James EK, Tabata S, Spaink HP. 2007. Characterization of genomic clones and expression analysis of the three types of superoxide dismutases during nodule development in *Lotus japonicus*. *Molecular Plant–Microbe Interactions* 20: 262–275.

Sánchez DH, Lippold F, Redestig H, Hannah MA, Erban A, Krämer U, Kopka J, Udvardi MK. 2008. Integrative functional genomics of salt acclimatization in the model legume *Lotus japonicus*. *Plant Journal* 53: 973–987.

Sandalio LM, Rodríguez-Serrano M, Romero-Puertas MC, del Río LA. 2008. Imaging of reactive oxygen species and nitric oxide *in vivo* in plant tissues. *Methods in Enzymology* 440: 397–409.

Sasaki T, Yamamoto Y, Ezaki B, Katsuhara M, Ahn SJ, Ryan PR, Delhaize E, Matsumoto H. 2004. A wheat gene encoding an aluminum-activated malate transporter. *Plant Journal* 37: 645–653.

Sharma P, Dubey RS. 2007. Involvement of oxidative stress and role of antioxidative defense system in growing rice seedlings exposed to toxic concentrations of aluminum. *Plant Cell Reports* 26: 2027–2038.

Tashiro M, Fujimoto T, Suzuki T, Furihata K, Machinami T, Yoshimura E. 2006. Spectroscopic characterization of 2-isopropylmalic acid–aluminum (III) complex. *Journal of Inorganic Biochemistry* 100: 201–205.

Tice KR, Parker DR, DeMason DA. 1992. Operationally defined apoplastic and symplastic aluminum fractions in root tips of aluminum-intoxicated wheat. *Plant Physiology* 100: 309–318.

Wang W, Vinocur B, Shoseyov O, Altman A. 2004. Role of plant heat-shock proteins and molecular chaperones in the abiotic stress response. *Trends in Plant Science* 9: 244–252.

Watt DA. 2003. Aluminium-responsive genes in sugarcane: identification and analysis of expression under oxidative stress. *Journal of Experimental Botany* 54: 1163–1174.

Yamamoto Y, Kobayashi Y, Matsumoto H. 2001. Lipid peroxidation is an early symptom triggered by aluminum, but not the primary cause of elongation inhibition in pea roots. *Plant Physiology* 125: 199–208.

Yamasaki H, Abdel-Ghany SE, Cohu CM, Kobayashi Y, Shikanai T, Pilon M. 2007. Regulation of copper homeostasis by micro-RNA in *Arabidopsis*. *Journal of Biological Chemistry* 282: 16369–16378.

Yang Q, Wang Y, Zhang J, Shi W, Qian C, Peng X. 2007. Identification of aluminium-responsive proteins in rice roots by a proteomic approach: cysteine synthase as a key player. *Proteomics* 7: 737–749.

Zhen Y, Qi JL, Wang SS, Su J, Xu GH, Zhang MS, Miao L, Peng XX, Tian D, Yang YH. 2007. Comparative proteome analysis of differentially expressed proteins induced by Al toxicity in soybean. *Physiologia Plantarum* 131: 542–554.

Zhou S, Sauvé R, Thannhauser TW. 2009. Proteome changes induced by aluminium stress in tomato roots. *Journal of Experimental Botany* 60: 1849–1857.

Supporting Information

Additional supporting information may be found in the online version of this article.

Fig. S1 Experimental setting for plant growth and aluminum (Al) treatment.

Fig. S2 Independent component analysis for the visualization of changes of relative protein abundance in roots of *Lotus corniculatus* exposed to 0 (control), 10 or 20 µM Al.

Fig. S3 Steady-state mRNA levels of the *ALMT* gene in *Lotus corniculatus* roots exposed to 10 or 20 µM Al.

Table S1 Effects of aluminum (Al) stress on the contents of nutrient elements in *Lotus corniculatus* roots

Table S2 Identification by proteomic analysis of peroxidases and glutathione *S*-transferases (GSTs) responsive to aluminum (Al) stress in *Lotus corniculatus* roots

Please note: Wiley–Blackwell are not responsible for the content or functionality of any supporting information supplied by the authors. Any queries (other than missing material) should be directed to the *New Phytologist* Central Office.